Accepted Manuscript

A hydrogen peroxide sensor based on TNM functionalized reduced graphene oxide grafted with highly monodisperse Pd nanoparticles

Sait Bozkurt, Berna Tosun, Betül Sen, Süleyman Akocak, Aysun Savk, Mehmet Faruk Ebeoğlugil, Fatih Sen

PII: S0003-2670(17)30855-3

DOI: 10.1016/j.aca.2017.07.051

Reference: ACA 235353

To appear in: *Analytica Chimica Acta*

Received Date: 13 April 2017

Revised Date: 13 July 2017

Accepted Date: 21 July 2017

Please cite this article as: S. Bozkurt, B. Tosun, B. Sen, S. Akocak, A. Savk, M.F. Ebeoğlugil, F. Sen, A hydrogen peroxide sensor based on TNM functionalized reduced graphene oxide grafted with highly monodisperse Pd nanoparticles, *Analytica Chimica Acta* (2017), doi: 10.1016/j.aca.2017.07.051.

GRAPHICAL ABSTRACT

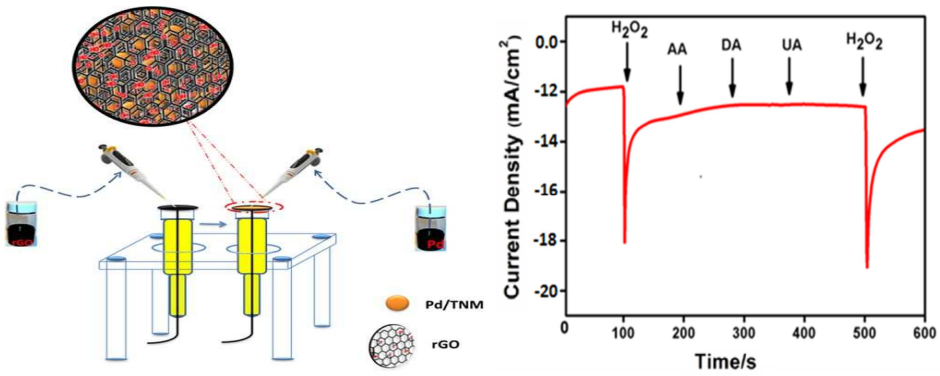

A hydrogen peroxide sensor based on TNM functionalized reduced graphene oxide grafted with highly monodisperse Pd nanoparticles

Sait Bozkurt [‡a], Berna Tosun [‡a, b], Betül Sen [a], Süleyman Akocak [a,c] , Aysun Savk [a] , Mehmet Faruk Ebeoğlugil [b] and Fatih Sen*[a]

[a] Sen Research Group, Department of Biochemistry, Faculty of Arts and Science, Dumlupınar University, Evliya Çelebi Campus, 43100 Kütahya, Turkey.

[b] Department of Material Science and Engineering, Faculty of Engineering, Dumlupınar University, Evliya Çelebi Campus, 43100 Kütahya, Turkey.

[c] Department of Pharmaceutical Chemistry, Faculty of Pharmacy, Adıyaman University, Adıyaman, Turkey.

* Corresponding author: fatih.sen@dpu.edu.tr

[‡] These authors equally contributed to this work.

Abstract

Adressed herein, we report the synthesis and characterization of a tert-nonyl mercaptan (TNM) funtionalized reduced graphene oxide (rGO) supported palladium (Pd) nanoparticles (NPs) (Pd/TNM@rGO) as electrochemical sensor. The highly monodisperse Pd/TNM@rGO nanocomposite was applied for electrochemical determination of hydrogen peroxide (H_2O_2) at a potential range of -0.6 to +0.8 V. The Pd/TNM@rGO sensor demonstrated very high activity, sensitivity, reusability and durability toward H_2O_2 sensing. The well dispersed Pd/TNM@rGO nanocomposite has been characterized by using several analytical tecniques such as, X-ray photoelectron spectroscopy (XPS), transmission electron microscopy (TEM), electron energy loss spectroscopy (EELS) and electrochemical impedance spectroscopy (EIS). The catalytic performance of prepared biosensor was also characterized by using cyclic voltammetry (CV) and chronoamperometry (CA) methods. The proposed H_2O_2 biosensor showed a broad linear range up to 12 mM, and a very low detection limit of 0.0025 µM, with a quick response time of less than 10 s. Additionally, the biosensor exhibited great capability, reproducibility and durability for the examination of H_2O_2.

Keywords: EIS, H_2O_2 sensor, Highly monodisperse, Pd nanomaterial, TNM functionalization.

1. Introduction

Carbon materials like graphene, carbon nanotubes etc are recently received significant attention as an attractive supporting material because of its unique properties and employed to different areas [1-6]. On the other hand, carbon materials especially graphene have also potential applications towards electrochemical applications by forming advanced carbon materials [7-15]. The graphene can be fabricated in a large quantities by using several different techniques which are adaptable and scalable to various types of applications. Carbon nanotubes (CNT) can also be given as a great examples of graphene frameworks for the impressive production of graphene [16-23]. More recently, the straightforward, green, and quick electrochemical methods for reducing GO were created independently by some researchers [24-33]. All the more vitally, the oxygen containing functional groups in the graphene oxide can be reduced by electrochemical methods to overcome energy barriers [24-30]. Electrochemical sensors which are obtained by electrochemical reduction of GO (rGO) has been applied for NADH, ascorbic acid, uric acid, H_2O_2, uric acid and dopamine etc. [34-39]. From this organic compounds, H_2O_2 attracted much attention because of wide range of applications in different fields such as food security, pharmaceuticals, environmental protection, fuel cells, and paper industry [40-42]. Noble nanoparticles (NPs) were also extensively studied as an electrocatalytic sensing of H_2O_2 [43-44] because of their enhanced catalytic performances. The enhanced catalytic performances of the metal–rGO interactions can be attributed to their excellent conductivity, fast electron transfer, their quantum size effect, reusability and high stability properties. For this reason, In current study, we report the synthesis of reduced GO with tert-nonyl mercaptan (TNM) (rGO–TNM), based Pd NPs (Pd/TNM@rGO). These NPs were fully characterized by using several analytical methods such as X-ray photoelectron spectroscopy (XPS), Raman spectroscopy, transmission electron microscopy (TEM),and electron energy loss spectroscopy (EELS) [45]. After that, the glassy carbon electrodes (GCEs) were modified by using these proposed Pd/TNM@rGO materials and used as a H_2O_2 biosensors with electrochemical measurements (CV and CA). The highly uniform well dispersed Pd/TNM@rGO nanomaterials have been simply synthesized, and indicated outstanding performance for sensing of H_2O_2. These nanomaterials have been used as a enzyme-free biosensors for the efficient determination of H_2O_2. The synergistic effect of metal, TNM and rGO caused the modifications of electron density in the nanomaterial and as a result enhanced catalytic activity of our newly designed biosensor for the determination of H_2O_2.

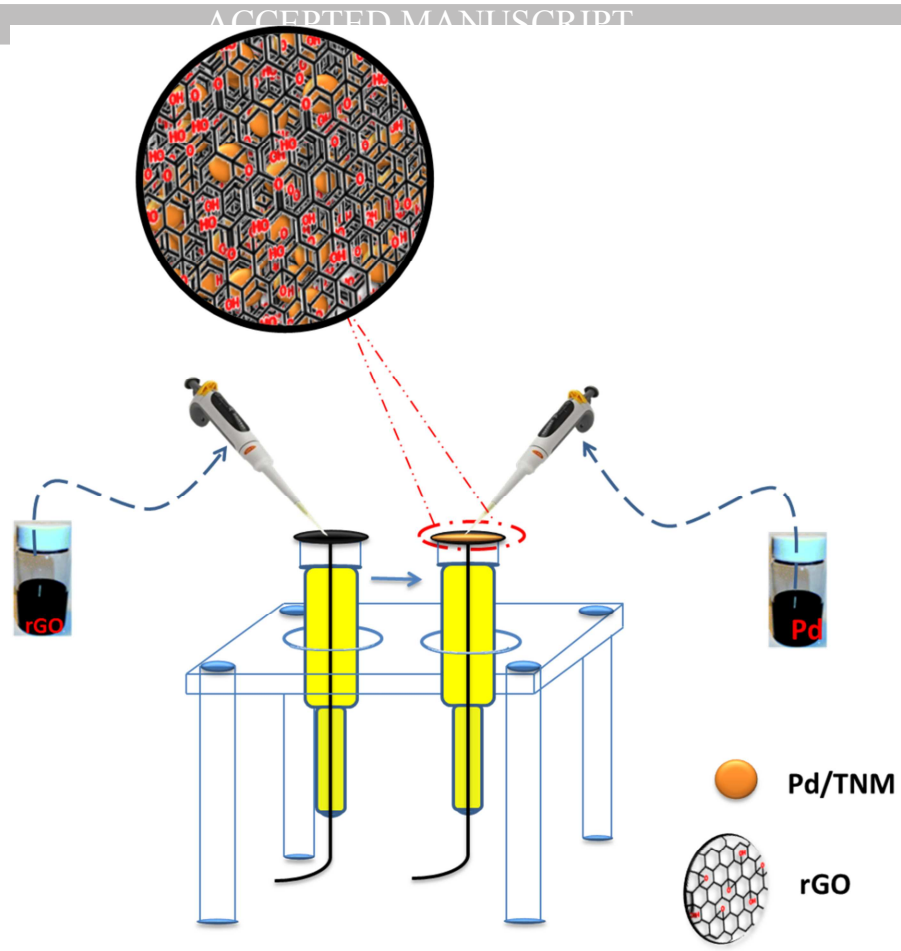

Scheme 1. The general mechanism of the synthesis of Pd/TNM@rGO

2. Experimental

2.1 Chemicals

Graphite powder (~325 mesh, 99.999%), potassium tetra- chloropalladate (K_2PdCl_4), sodium borohydride ($NaBH_4$), tert-nonyl mercaptan (TNM) were obtained from Aldrich. Membrane filters (pore size 0.45 µm, diameter 47 mm) were purchased from Tokyo Roshi Kaisha, Ltd. All other reagents were of analytical grade and were used without further purification. Phosphate buffer solution (PBS) was prepared with 0.1 M $NaHPO_4$; and the pH was adjusted with 0.1 M NaOH and 0.1 M H_3PO_4. Double distilled water was used in the preparation of the aqueous electrolyte solutions.

2.2 Instruments

A three-electrode assembled cell was employed. A GCE (3.0 mm diameter) was made with a working electrode, platinum-wire counter electrode, and an Ag/AgCl (3.0 M NaCl) reference electrode. Electrochemical characterization by CV, CA and electrochemical impedance spectroscopy (EIS) were performed using a Reference 3000 potentiostate system (Gamry, USA). TEM samples were made

ready by dropping of 0.5 mg/mL ethanol solution of the prepared catalysts with an activated carbon support on a carbon covered 400-mesh copper grid, and then the solvent was vaporized. Elimination of excess solution was performed with an adsorbent paper and the sample was dried under vacuum at room temperature before analysis. TEM analysis was carried out by a JEOL 200 kV. More than 300 particles were calculated to get the integrated information about the overall distribution of Pd-based catalyst sample.

During X-ray Photoelectron Spectroscopy (XPS) analysis, Specs spectrometer was employed and as an X-ray source Kα lines of Mg (1253.6 eV, 10 mA) was used. Sample preparation was done by depositing the catalyst on Cu double-sided tape (3M Inc.). C 1s line at 284.6 eV was selected as a reference point and all XPS peaks were fitted using a Gaussian function.

XRD analysis were performed with a Panalytical Empyrean diffractometer with Ultima+theta–theta high resolution goniometer, having an X-ray generator (Cu K∞ radiation, k = 1.54056 Å) and operating condition of 40 kV and 40 mA.

Raman spectrum was carried out using an in via Raman microprobe (Renishaw Instruments) with 514 nm laser excitation.

2.3 Preparation of Pd/TNM@rGO

The modified Hummers'method was applied to produce graphene oxide from graphite [46]. Briefly, the GO (50 mg) was dispersed in THF (10 mL) in round-bottom flask followed by the addition of tert-nonyl mercaptan (TNM) (1 mg/mL). It was then stirred for 1h at room temperature and after that ultrasonicated for 1 h. The mixture was filtrated to separate of dark brown material from solution and washed with EtOH to clean up the final product and was dried in a vacuum oven at 50 ◦C for 24h. $NaBH_4$ was used as an efficient material to reduce and support Pd nanoparticles on rGO-TNM. The sonication method was employed to combine of 30 mg rGO–TNM and K_2PdCl_4 (0.25% w/v) in the mixture with 30 mL of deionized water, and followed by vigorous stirring at 55 ◦C for 12 h. Afterward, every 5 min 100 µL of $NaBH_4$ solution was injected to solution and after that repeatedly washed with deionized water. Pd/TNM@rGO NPs have been dried in a vacuum chamber. Electrochemical preparation and fabrication of modified electrode were given in detail in supporting information.

2.4 Electrochemical preparation and fabrication of modified electrode

Firstly, the GCE surfaces were exceedingly cleaned with alumina paste, and were then washed successively with distilled water, and flushed with methanol in ultrasonic bath. The pre-cleaned GCEs

were sonicated for 5 min in a water bath and then covered with a 10 µL suspension of Pd/TNM@rGO NPS and dried at room temperature. The produced electrode was indicated as Pd/TNM@rGO/GCE. 5 successive cyclic voltammograms were performed in the potential range of -0.6 V to +0.8 in an electrochemical cell containing 0.1 M PBS solution (pH 7). The subsequent Pd/TNM@rGO/GCE was washed several times with distilled water and then afterward each analysis.

3. Results and discussion

3.1 Characterization of Pd/TNM@rGO NPs

The preliminary characterizations of well dispersed Pd/TNM@rGO were carried out by using XRD, TEM, HR-TEM, EELS, Raman and XPS. The X-ray diffraction (XRD) spectra was studied to define the crystal structure and average crystallite size of highly monodisperse Pd/TNM@rGO and was illustrated in Figure 1(a). The peak at around 24.8^{o} is assigned to the carbon (002) plane of rGO. Moreover, four reflactions at around 2θ = 40.2° , 46.8° , 68.3° and 82.3° attributable to Pd (111), (200), (220) and (311) crystal planes of a face centered cubic (fcc) structures of palladium (JCPDS-ICDD, Card No. 04-802), respectively. To calculate the lattice parameter (αPd) values of the metal particles, the Pd (220) diffraction peak of the prepared catalyst Pd/TNM@rGO was used. The lattice constant values of uniformly dispersed Pd/TNM@rGO nanoclusters was obtained to be 3.887 Å using the following equation that is in good aggrement with 3.890 Å for pure Pd.

$$\sin\theta = \frac{\lambda\sqrt{h^2+k^2+l^2}}{2a} \text{ (for a cubic structure)} \qquad \text{(Eq.1)}$$

Furthermore, the average crysallite palladium particle size of well dispersed Pd/TNM@rGO have been calculated 3.57 ± 0.38 nm using Debye Scherer equation [47-50].

Raman spectroscopy is additionally a successful and effective technique to recognize the ordered and disordered structure of carbon in carbonaceous materials. The Raman spectroscopic analysis was performed for GO, rGO and Pd/TNM@rGO are appeared in Fig. 1b. Two prominent scattering peaks located at 1351 and 1575 cm^{-1} can be assigned to the D-band (E2g phonon of sp^2 carbon atoms) and the G-band (breathing mode of κ-point phonons of A1g symmetry), respectively. The intensity ratio of D to G band (ID/IG) generally used to evaluate the degree of modification or defects of GO and rGO. In this work, the ID/IG values of GO, rGO and Pd/TNM@rGO are 0.98, 1.04 and 1.10, respectively which demonstrates that the Pd has functionalized with the TNM@rGO.

The high resolution electron micrograph (HRTEM) and particle size histogram of Pd/TNM@rGO show the highly monodisperse morphology of the sensors as indicated in (Figure 1 (c,d,e)). The average particle sizes of Pd/TNM@rGO were found to be 3.89 ± 0.43 nm and a uniform distribution of the

nanoparticles with a very narrow range on rGO was detected. The HRTEM results also revealed that most of the particles were in a spherical shape, and no agglomerations were observed in the prepared sensors. Moreover, as shown in Fig 1(c), the representative atomic lattice fringes obtained by HRTEM was found to be 0.22 nm for Pd/TNM@rGO which is in good agreement with nominal Pd value (Celik et al; 2016). Besides, the EELS elemental color-map the EELS line profile scanned on the arrow shown in HRTEM for palladium indicates the existence of Pd in prepared as shown in Fig 1 (d and e).

X-ray photoelectron spectroscopy (XPS) was used to evaluate the surface elemental compositions, and chemical oxidation states of metals in the Pd/TNM@rGO NPs. XPS (Fig. 1 g and h) show that the core level of Pd 3d5/2 was at 335.3 eV, indicating that most of the Pd atoms were present in the metallic state. These results display that Pd is present as elements in Pd/TNM@rGO nano clusters rather than oxygen-containing compounds. As illustrated in the Figure 1 (g and h), the Pd (II) peak at 338.5 eV may be caused by the surface oxidation and/or chemisorption of environmental oxygen during the preparation process.

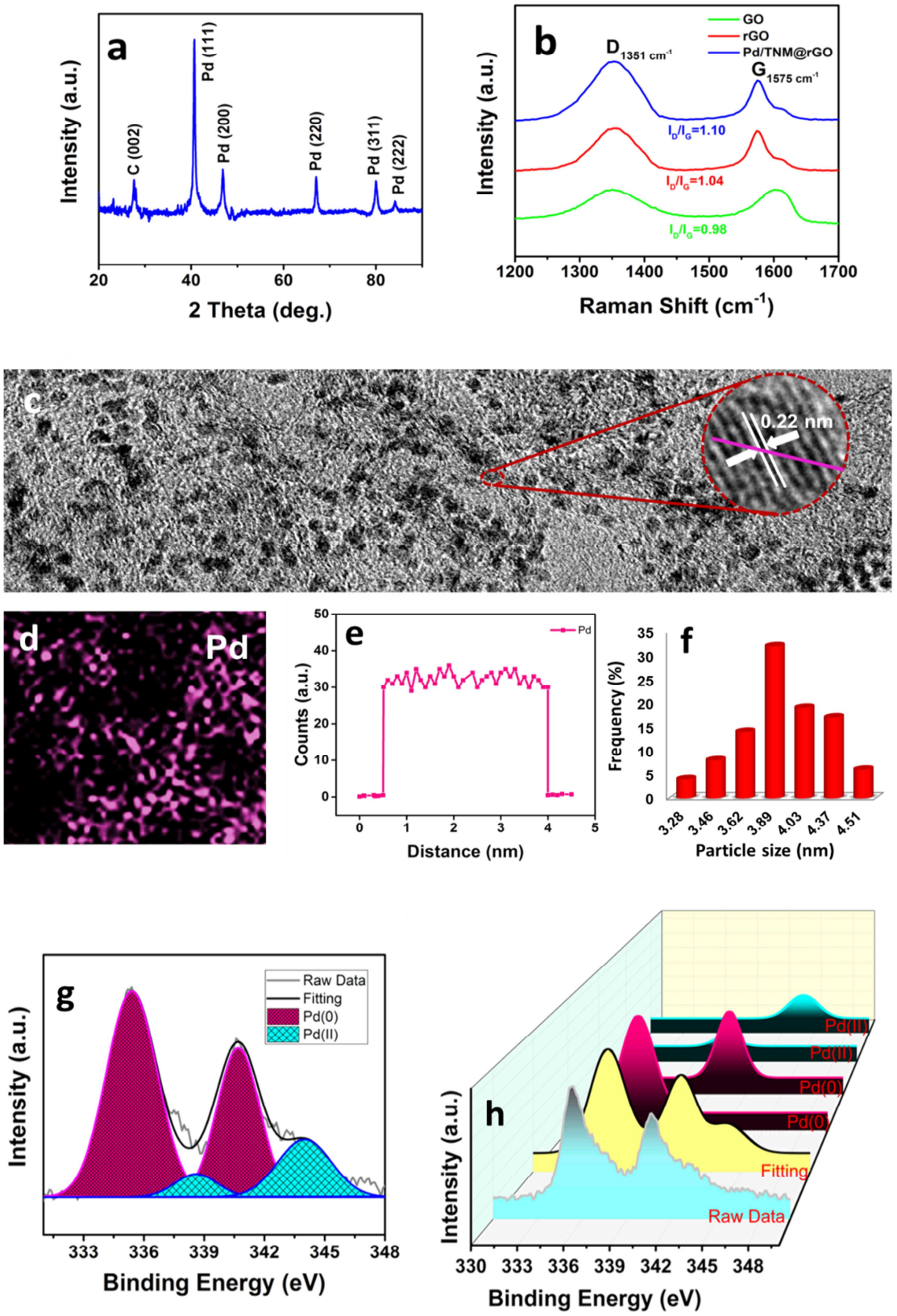

Fig.1. XRD pattern (a) Raman spectra (b) Transition electron micrograph (c) the EELS elemental color-map (d) the EELS line profile of palladium (e) particle size histogram of Pd/TNM@rGO NPs (f), Pd 3d XPS spectra (g), 3D XPS view of Pd/TNM@rGO (h).

3.2. EIS measurement

As an illustrated in Figure 2, the redox couple of 5.0 mM H_2SO_4 (1:1) has been achieved at 10^5Hz – 10^{-2}Hz by using Nyquist plot. The bare glassy carbon electrode (GCE) exhibited an enormous semicircle of up to 2.8 kΩ diameter (Fig. 2) compared to the TNM@rGO-GCE and Pd-TNM@rGO-GCE. After addition of rGO to the GCE surfaces significantly increased the electron transfer resistance (Fig. 2), and it can be explained that rGO prevents interfacial electron transfer due to the disturbed sp^2 bonding systems [32-33]. As shown in Fig. 2 after addition of rGO–TNM and the following addition of Pd NPs diminished resistance. Besides, Pd/TNM@rGO nanocomposites have increased conductivity and and permitted electron transfer more and more compared to the other modified electrodes [48].

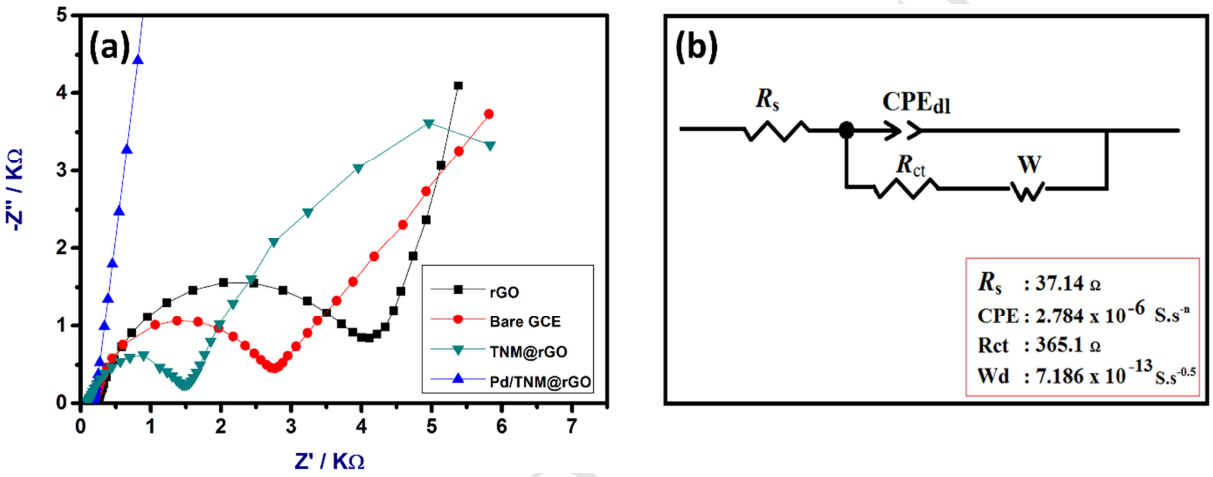

Fig.2. Electrochemical impedance spectra of the Nyquist plots of bare GCE, rGO, TNM@rGO and Pd/TNM@rGO modified GCE, in 5.0 mM H_2SO_4.

3.3. Electrochemical determination of H_2O_2

The electrochemical performance of the rGO/GCE and Pd/TNM@rGO/GCE nanocomposites were investigated using cyclic voltammograms for 5 mM H_2O_2 in 0.1 M PBS (pH 7.4) as illustrated in Fig. 3. While rGO /GCE demonstrated a highly low current density, Pd/TNM@rGO /GCE indicated very high current density. The electrochemical reactions mechanism was already given in literature for the existence of H_2O_2 as indicated in Fig. 3. [49]. It can be suggested that the electrocatalytic reduction of H_2O_2 can only take place efficiently by the help of Pd/TNM@rGO nanocomposites.

$H_2O_2 + e^- \rightarrow (OH)_{ads} + OH^-$ (by the help of Pd/TNM@rGO) (Eq. 2)

$H_2O_2 + H^+ + OH_{(ads)} + e^- \rightarrow 2\ OH_{(ads)} + H_2O$ (by the help of Pd/TNM@rGO) (Eq. 3)

In this mechanism, the reduction of the first H_2O_2 molecule provides the initial source of $OH_{(ads)}$ at a small overpotential, which also allow the reduction of the secondary H_2O_2 molecule at a faster rate. This process also results in the accumution of $OH_{(ads)}$ intermediates on the electrode surface, provided that the reduction of H_2O_2 takes place continuously [49].

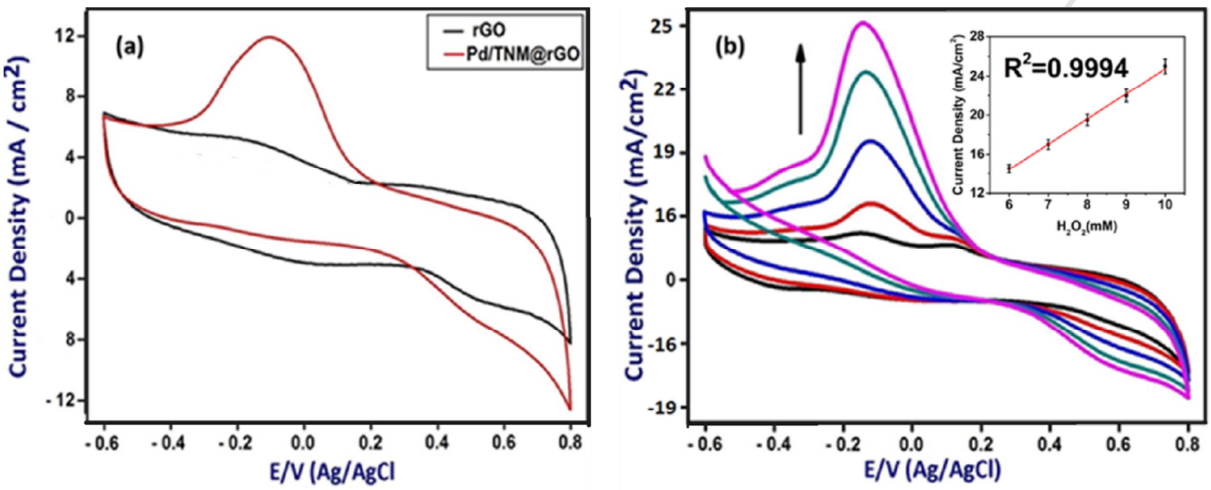

Fig.3. Cyclic voltammograms of rGO and Pd-TNM@rGO in 0.1 M PBS, with 5 mM H_2O_2 (a) 6, 7, 8, 9 and 10 mM H_2O_2 addition (b). Scan rate: 50 mV/s

The Pd/TNM@rGO modified electrode displayed significantly higher efficiency and electrocatalytic activity compared to the rGO /GCE because of easier electron transfer of Pd/TNM@rGO /GCEs. The amperometric current-time curves of rGO /GCE and Pd/TNM@rGO /GCE for progressive augmentations of 1 mM H_2O_2 at an employed potential of -0.1 V are displayed in Fig. 4. An employed potential of −0.1 V on the Pd/TNM@rGO /GCE demonstrated a decent of ca. 3.678 mA mM^{-1} cm^{-2} (3.0 mm diameter). The response current density versus H_2O_2 concentration demonstrated great linear range up to 12 mM, and steady-state signals were accomplished within very short times. Fig. 4 also illustrates that the sensitivity of Pd/TNM@rGO /GCE was higher than the other prepared ones, which additionally exhibited the extra catalytic effect offered by the Pd/TNM@rGO.

Chronoamperometry (CA) was also utilized to decide the limit of detection for the prepared sensors, with inspecting up to 12 mM H_2O_2 (Fig. 4). Pd/TNM@rGO /GCE indicated linear current density ranges at concentrations of 1 mM–12 mM.

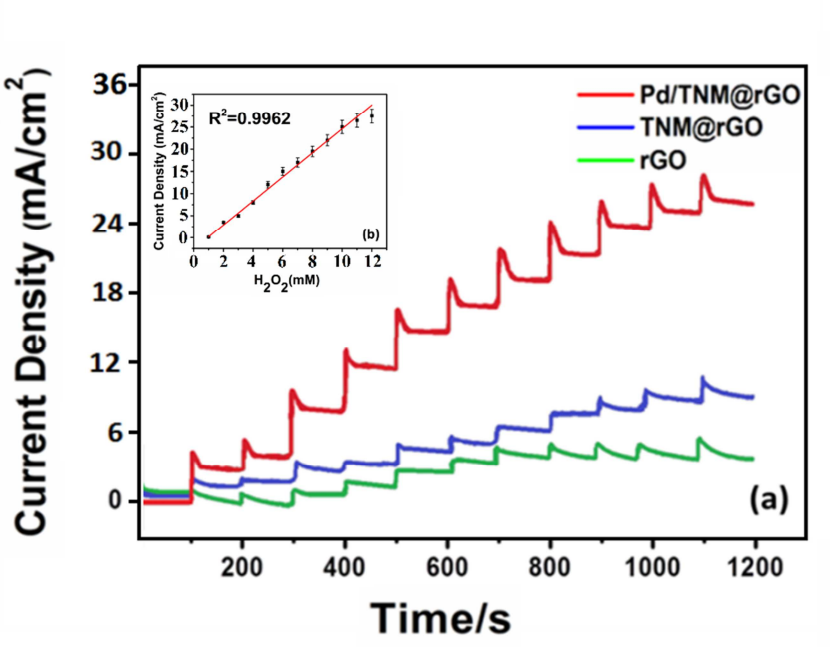

Fig.4. Amperometric responses rGO, TNM@rGO and Pd/TNM@rGO to 1–12 mM H_2O_2 in 0.1 M PBS at pH 7.4 at applied potentials of −0.1 V (a) and Calibration Plot of Pd/TNM@rGO for 1-12 mM H_2O_2 (b).

3.4. Stability, selectivity and repeatability of H_2O_2 biosensor

In the determination of real samples, some common electro-active substances such as, ascorbic acid (AA), dopamine (DA) and uric acid (UA), were tested. As shown in Fig. 5, the responses to following addition of 1.0 mM H_2O_2, 0.15 mM AA, 0.2 mM dopamine, 0.5 mM UA, and 1.0 mM H_2O_2 were measured at −0.1 V. Interference concentrations have been used depending upon the endogenous levels of AA, dopamine, and UA (ca. 0.125 mM, 4.4 mM–6.6 mM, and 0.33 mM, respectively) in blood. As indicated in Fig. 5, these substances have negligible interference to H_2O_2 responses, which indicate the Pd/TNM@rGO nanocomposites exhibit the great selectivity to sensing of H_2O_2. The prepared biosensor demonstrated excellent repeatability, with low RSD (relative standard deviations) in response to 1 mM H_2O_2 of 5.12 % found for Pd/TNM@rGO /GCE, from five different electrodes.

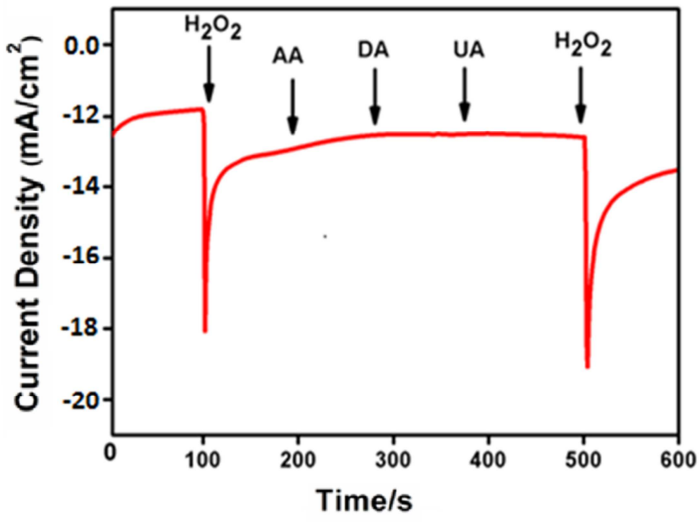

Fig.5. Amperometric response of Pd/TNM@rGO to the sequential addition of 1 mM H_2O_2, 0.15 mM ascorbic acid (AA), 0.2 mM dopamine (DA), 0.5 mM uric acid (UA), and 1 mM H_2O_2. Applied potential: −0.1 V.

Table 1: Comparison of rGO-based biosensors' activities and H_2O_2 detection

Types of electrode	Detection potential (V)	Sensitivity ($\mu A\ mM^{-1}\ cm^{-2}$)	Linear range (mM)	Detection limit (µM)	Ref.
ER–GNO/IL–SPE	–0.2	78.13	0.1×10^{-3}-2.0	0.05	[35]
rGO/ZnO/GCE	–0.38	1.34×10^{-2}	1.0×10^{-3} 2.25×10^{-2}	0.02	[36]
NF/CAT/rGO/GCE	–0.45	7.76	5×10^{-2}-1.91	-----	[50a]
PDDA/ERGO–ATP–Pd/GCE	–0.2	492.09	0.1×10^{-3}-10	0.016	[50b]
Pd/TNM@rGO NPs	-0.1	3678	Up To 12	0.0025	[This Work]
Pd@rGO NPs	-0.15	1052	Up To 10	0.010	[This Work]
Pd NPs	-0.2	476	Up To 8	0.021	[This Work]

3.5. Analytical Application of the Biosensor

The accuracy of the biosensor was evaluated by determining the recoveries of hydrogen peroxide in a disinfectant using a standard addition method. Corresponding experiments were carried out with the titration method and the results displayed good consistent and precision between the two methods, as listed in Table 2. As seen in Table 2, the results obtained by the biosensor are satisfactory, with the recovery ranging from 99.1% to 101.1 %.

Table 2. Recovery determination results (The average of three measurements).

Sample Number	Added H_2O_2 (mM)	Found H_2O_2 by current biosensor (mM)	Recovery by current biosensor (%)	Found H_2O_2 by titration method (mM)
1	0.2	0.821	101.1	0.812
2	0.6	1.264	100.6	1.256
3	1.2	1.814	99.1	1.830

4.Conclusions

As a result, the highly monodisperse Pd/TNM@rGO nanocomposites were prepared via a facile approach and they were fully characterized by several analytical methods such as, TEM, XPS, XRD, HR-TEM, and EELS. Besides, the electrocatalytic efficiency of newly prepared catalyst was studied by cyclic voltammetry and chronoamperometry techniques. The created electrochemical sensor Pd/TNM@rGO /GCE indicated great electro biosensing activity toward H_2O_2 determination. A highly monodisperse Pd/TNM@rGO was obtained with GO functionalized with TNM [TNM@rGO], and palladium supported NPs. The results show that the Pd/TNM@rGO electrode indicates great electrocatalytic biosensing performence towards hydrogen peroxide with good durability, high sensitivity, excellent reproducibility, good selectivity and very low detection limits. The unique structure, the specific interactions between Pd and TNM@rGO and their large surface area to volume ratio may lead to a one of the record electrosensing activity. Another advantegous feature of the Pd/TNM@rGO/GCE is its stability, as it showed great stability even it was kept under dry conditions for more than ten weeks. These great electrochemical sensing properties of Pd/TNM@rGO/GCE can be explained by the ultrasmall sizes, monodispersity and high Pd % surface of novel materials. Finally, the Pd/TNM@rGO amperometric H_2O_2 sensors could be promising enzyme-free electrocatalytic electrode material for electrochemical sensors towards the determination of H_2O_2.

5. References

[1] (a) G. Baskaya, Y. Yıldız, A. Savk, T.O. Okyay, S. Eris, H. Sert & F. Sen, Rapid, sensitive, and reusable detection of glucose by highly monodisperse nickel nanoparticles decorated functionalized multi-walled carbon nanotubes. Biosensors and Bioelectronics. 91 (2017) 728-733. (b) L. Wang, Y. Nemoto, & Y. Yamauchi, Direct synthesis of spatially-controlled Pt-on-Pd bimetallic nanodendrites with superior electrocatalytic activity. Journal of the American Chemical Society. 133 (25) (2011) 9674-9677. (c) J. Wang, H.B. Sun, H.Y. Pan, Y.Y. Ding, J.G. Wan, G.H. Wang, & M. Han, Detection of hydrogen peroxide at a palladium nanoparticle-bilayer graphene hybrid-modified electrode. Sensors and Actuators B: Chemical. 230 (2016) 690-696. (d) B. Celik, E. Erken, S. Eris, Y. Yıldız, B. Sahin, H. Pamuk, & F. Sen, Highly monodisperse Pt (0)@ AC NPs as highly efficient and reusable catalysts: the effect of the surfactant on their catalytic activities in room temperature dehydrocoupling of DMAB. Catalysis Science & Technology. 6(6) (2016) 1685-1692.

[2] N.M. Iverson, P.W. Barone, M. Shandell, L.J. Trudel, S.Sen, F.Sen, & N. Reuel, In vivo biosensing via tissue-localizable near-infrared-fluorescent single-walled carbon nanotubes. Nature nanotechnology. 8(11) (2013) 873-880. (b) E. Erken, H. Pamuk, Ö. Karatepe, G. Baskaya, H. Sert, O.M. Kalfa, & F. Sen, New Pt (0) nanoparticles as highly active and reusable catalysts in the C1–C3 alcohol oxidation and the room temperature dehydrocoupling of dimethylamine-borane (DMAB). Journal of Cluster Science 27(1) (2016) 9-23. (c) L. Wang, & Y. Yamauchi, Metallic nanocages: synthesis of bimetallic Pt–Pd hollow nanoparticles with dendritic shells by selective chemical etching. Journal of the American Chemical Society 135(45) (2013) 16762-16765. (d) J.J. He, J. Sunarso, Y. Zhu, Y. Zhong, J. Miao, W. Zhou, & Z. Shao, High-performance non-enzymatic perovskite sensor for hydrogen peroxide and glucose electrochemical detection. Sensors and Actuators B: Chemical. 244 (2017) 482-491. (e) A.A. Boghossian, F. Sen, B.M. Gibbons, S. Sen, S.M. Faltermeier, J.P. Giraldo, C.T. Zhang, J. Zhang, D.A. Heller, M.S. Strano, Advanced Energy Materials. 3 (7) (2013) 881-893.

[3] Y. Yıldız, S. Kuzu, B. Sen, A. Savk, S. Akocak, & F.Sen, Different ligand based monodispersed Pt nanoparticles decorated with rGO as highly active and reusable catalysts for the methanol oxidation. International Journal of Hydrogen Energy. 42(18) (2017) 13061-13069 (b) V. Malgras, H. Ataee-Esfahani, H. Wang, B. Jiang, C. Li, K.C. Wu, & Y.Yamauchi, Nanoarchitectures for mesoporous metals. Advanced Materials. 28(6) (2016) 993-1010. (c) F. Sen, A.A. Boghossian, S. Sen, Z.W. Ulissi, J. Zhang, & M.S. Strano, Observation of oscillatory surface reactions of riboflavin, trolox, and singlet oxygen using single carbon nanotube fluorescence spectroscopy. ACS nano. 6(12) (2012) 10632-10645.

[4] (a) Y. Yıldız, H. Pamuk, Ö. Karatepe, Z. Dasdelen, & F. Sen, Carbon black hybrid material furnished monodisperse platinum nanoparticles as highly efficient and reusable electrocatalysts for formic acid electro-oxidation. RSC Advances. 6(39) (2016) 32858-32862. (b) R. Ayranci, G. Baskaya, M. Güzel, S. Bozkurt, F. Sen, & M. Ak, Carbon based nanomaterials for high performance optoelectrochemical systems. ChemistrySelect. 2(4) (2017) 1548-1555. (c) Y. Yıldız, E. Erken, H. Pamuk, H. Sert, & F. Sen, Monodisperse Pt nanoparticles assembled on reduced graphene oxide: highly efficient and reusable catalyst for methanol oxidation and dehydrocoupling of dimethylamine-borane (DMAB). Journal of nanoscience and nanotechnology. 16(6) (2016) 5951-5958.

[5] S. Sen, F. Sen, A.A. Boghossian, J. Zhang, & M.S. Strano, Effect of reductive dithiothreitol and trolox on nitric oxide quenching of single-walled carbon nanotubes. The Journal of Physical Chemistry C. 117(1) (2012) 593-602. (b) R. Ayranci, G. Baskaya, M. Güzel, S. Bozkurt, F. Sen, & M. Ak, Carbon based nanomaterials for high performance optoelectrochemical systems. ChemistrySelect. 2(4) (2017) 1548-1555. (c) E. Erken, , Y. Yıldız, B. Kilbaş, & F. Sen, Synthesis and characterization of nearly monodisperse Pt nanoparticles for C1 to C3 alcohol oxidation and dehydrogenation of dimethylamine-borane (DMAB). Journal of nanoscience and nanotechnology. 16(6) (2016) 5944-5950.

[6] (a) B. Aday, H. Pamuk, M. Kaya, & F. Sen, Graphene oxide as highly effective and readily recyclable catalyst using for the one-pot synthesis of 1, 8-dioxoacridine derivatives. Journal of nanoscience and nanotechnology. 16(6) (2016) 6498-6504. (b) Y. Yildiz, T.O. Okyay, B. Sen, B. Gezer, S. Kuzu, A.Savk, & F.Sen Highly monodisperse Pt/Rh nanoparticles confined in the graphene oxide for highly efficient and reusable sorbents for methylene blue removal from aqueous solutions. ChemistrySelect. 2(2) (2017) 697-701.

[7] S.Yang, G. Li, G. Wang, J. Zhao, M. Hu, & L. Qu, A novel nonenzymatic H_2O_2 sensor based on cobalt hexacyanoferrate nanoparticles and graphene composite modified electrode. Sensors and Actuators B: Chemical. 208 (2015) 593-599.

[8] F. Lorestani, Z.P. Shahnavaz, Y. Alias, & N.S. Manan, One-step hydrothermal green synthesis of silver nanoparticle-carbon nanotube reduced-graphene oxide composite and its application as hydrogen peroxide sensor. Sensors and Actuators B: Chemical. 208 (2015) 389-398.

[9] L.J. Cote, F. Kim, J. Huang, Langmuir−Blodgett assembly of graphite oxide single layers. Journal of the American Chemical Society. 131(3) (2008) 1043-1049.

[10] D.A Dikin, S. Stankovich, E.J. Zimney, R.D. Piner, G.H. Dommett, G. Evmenenko, & R.S. Ruoff, Preparation and characterization of graphene oxide paper. Nature. 448(7152) (2007) 457-460.

[11] J. Xia, F. Chen, J. Li, & N.N Tao, Measurement of the quantum capacitance of graphene. Nature nanotechnology. 4(8) (2009) 505-509.

[12] L. Tang, Y. Wang, Y. Li, H. Feng, J. Lu, & J. Li, Preparation, structure, and electrochemical properties of reduced graphene sheet films. Advanced Functional Materials. 19(17) (2009) 2782-2789.

[13] Y. Wang, Y. Li, L. Tang, J. Lu, & J. Li, Application of graphene-modified electrode for selective detection of dopamine. Electrochemistry Communications. 11(4) (2009) 889-892.

[14] H.A. Becerril, J. Mao, Z. Liu, R.M. Stoltenberg, Z. Bao, & Y. Chen, Evaluation of solution-processed reduced graphene oxide films as transparent conductors. ACS nano. (2008) 2(3) 463-470.

[15] K.A. Mkhoyan, A.W. Contryman, J. Silcox, D.A. Stewart, G. Eda, C. Mattevi, & M. Chhowalla, Atomic and electronic structure of graphene-oxide. Nano letters. 9(3) (2009) 1058-1063.

[16] W. Zhao, C. Song, & P.E. Pehrsson, Water-soluble and optically pH-sensitive single-walled carbon nanotubes from surface modification. Journal of the American Chemical Society. 124(42) (2002) 12418-12419.

[17] J. Wang, G. Liu, & M.R. Jan, Ultrasensitive electrical biosensing of proteins and DNA: carbon-nanotube derived amplification of the recognition and transduction events. Journal of the American Chemical Society. 126(10) (2004) 3010-3011.

[18] S. Lijima, Helical microtubules of graphitic carbon. Nature. 354 (1991) 56–58.

[19] K. Gong, M. Zhang, Y. Yan, L. Su, L. Mao, S. Xiong, & Y. Chen, Sol− gel-derived ceramic− carbon nanotube nanocomposite electrodes: tunable electrode dimension and potential electrochemical applications. Analytical chemistry. 76(21) (2004) 6500-6505.

[20] J. Wang, M. Musameh, & Y. Lin, Solubilization of carbon nanotubes by Nafion toward the preparation of amperometric biosensors. Journal of the American Chemical Society. 125(9) (2003) 2408-2409.

[21] M.R. Akhgar, H. Beitollahi, M. Salari, H. Karimi-Maleh, & H. Zamani, Fabrication of a sensor for simultaneous determination of norepinephrine, acetaminophen and tryptophan using a modified carbon nanotube paste electrode. Analytical Methods. 4(1) (2012) 259-264.

[22] U. Yogeswaran, S. Thiagarajan, & S.M. Chen, Nanocomposite of functionalized multiwall carbon nanotubes with nafion, nano platinum, and nano gold biosensing film for simultaneous determination of ascorbic acid, epinephrine, and uric acid. Analytical biochemistry. 365(1) (2007) 122-131.

[23] A.A. Ensafi, H. Karimi-Maleh, S. Mallakpour, & B. Rezaei, Highly sensitive voltammetric sensor based on catechol-derivative-multiwall carbon nanotubes for the catalytic determination of captopril in patient human urine samples. Colloids and Surfaces B: Biointerfaces. 87(2) (2011) 480-488.

[24] Y. Zhang, Y.Cheng, Y. Zhou, B. Li, W. Gu, X. Shi, & Y. Xian, Electrochemical sensor for bisphenol A based on magnetic nanoparticles decorated reduced graphene oxide. Talanta. 107 (2013) 211-218.

[25] W. Zhou, C. Sun, Y. Zhou, X. Yang, & W. Yang, A facial electrochemical approach to determinate bisphenol A based on graphene-hypercrosslinked resin MN_20_2 composite. Food chemistry. 158 (2014) 81-87.

[26] L. Zhou, J. Wang, D. Li, & Y. Li, An electrochemical aptasensor based on gold nanoparticles dotted graphene modified glassy carbon electrode for label-free detection of bisphenol A in milk samples. Food chemistry. 162 (2014) 34-40.

[27] H.Yin, L. Cui, Q. Chen, W. Shi, S. Ai, L. Zhu, & L. Lu, Amperometric determination of bisphenol A in milk using PAMAM–Fe_3O_4 modified glassy carbon electrode. Food Chemistry. 125(3) (2011) 1097-1103.

[28] M. Najafi, M.A. Khalilzadeh, & H. Karimi-Maleh, A new strategy for determination of bisphenol A in the presence of Sudan I using a ZnO/CNTs/ionic liquid paste electrode in food samples. Food chemistry. 158 (2014) 125-131.

[29] B.Yu, Y. Liu, J.Zhang, T. Hai, B. Li. P. Lu, & Y. Jing, Electrochemical Analysis of Nicotine Based on Multi-Walled Carbon Nanotube/Graphene Composite. Int. J. Electrochem. Sci. 11 (2016) 4979-4987.

[30] (a) Y. Zheng, L. Fu, F. Han, A. Wang, W. Cai, J. Yu, & F. Peng, Green biosynthesis and characterization of zinc oxide nanoparticles using Corymbia citriodora leaf extract and their photocatalytic activity. Green Chemistry Letters and Reviews. 8(2) (2015) 59-63. (b) Y. Zheng, L. Fu, A. Wang, F. Peng, J. Yang, & F. Han, One-pot hydrothermal preparation of SnO_2–ZnO nanohybrids for simultaneous electrochemical detection of catechol and hydroquinone. Sensor Letters. 13(10) (2015) 878-882. (c) Y. Zheng, A. Wang, H. Lin, L. Fu, & W. Cai, A sensitive electrochemical sensor for direct phoxim detection based on an electrodeposited reduced graphene oxide–gold nanocomposite. RSC Advances. 5(20) (2015) 15425-15430.

[31] Z. Wang, X. Zhou, J. Zhang, F. Boey, & H. Zhang, Direct electrochemical reduction of single-layer graphene oxide and subsequent functionalization with glucose oxidase. The Journal of Physical Chemistry C. 113 (32) (2009) 14071-14075.

[32] H.P. Cong, J.F. Chen, & S.H. Yu, Graphene-based macroscopic assemblies and architectures: an emerging material system. Chemical Society Reviews. 43(21) (2014) 7295-7325.

[33] C.T. Hsieh, Y.Y. Liu, & A.K. Roy, Pulse electrodeposited Pd nanoclusters on graphene-based electrodes for proton exchange membrane fuel cells. Electrochimica Acta. 64 (2012) 205-210.

[34] H. Xiong, & B. Jin, The electrochemical behavior of AA and DA on graphene oxide modified electrodes containing various content of oxygen functional groups. Journal of electroanalytical chemistry. 661(1) (2011) 77-83.

[35] J. Ping, Y. Wang, K. Fan, J. Wu, & Y. Ying, Direct electrochemical reduction of graphene oxide on ionic liquid doped screen-printed electrode and its electrochemical biosensing application. Biosensors and Bioelectronics. 28(1) (2011) 204-209.

[36] S. Palanisamy, S.M. Chen, & R. Sarawathi, A novel nonenzymatic hydrogen peroxide sensor based on reduced graphene oxide/ZnO composite modified electrode. Sensors and Actuators B: Chemical. 166 (2012) 372-377.

[37] J. Yang, S. Deng, J. Lei, H. Ju, & Gunasekaran, S. Electrochemical synthesis of reduced graphene sheet–AuPd alloy nanoparticle composites for enzymatic biosensing. Biosensors and Bioelectronics. 29(1) (2011) 159-166.

[38] J. Luo, H. Zhang, S. Jiang, J. Jiang, & X. Liu, Facile one-step electrochemical fabrication of a non-enzymatic glucose-selective glassy carbon electrode modified with copper nanoparticles and graphene. Microchimica Acta. 177(3-4) (2012) 485-490.

[39] P. Si, H. Chen, P. Kannan, & D.H. Kim, Selective and sensitive determination of dopamine by composites of polypyrrole and graphene modified electrodes. Analyst. 136(24) (2011) 5134-5138.

[40] J.M. You, Y.N. Jeong, M.S. Ahmed, S.K. Kim, H.C. Choi, & S. Jeon, Reductive determination of hydrogen peroxide with MWCNTs-Pd nanoparticles on a modified glassy carbon electrode. Biosensors and Bioelectronics. 26(5) (2011) 2287-2291.

[41] X. Lu, J. Zhou, W. Lu, Q. Liu, & J. Li, Carbon nanofiber-based composites for the construction of mediator-free biosensors. Biosensors and Bioelectronics. 23(8) (2008) 1236-1243.

[42] L. Wang, & E. Wang, A novel hydrogen peroxide sensor based on horseradish peroxidase immobilized on colloidal Au modified ITO electrode. Electrochemistry Communications. 6(2) (2014) 225-229.

[43] Y. Liu, D. Wang, L. Xu, H. Hou, & T. You. A novel and simple route to prepare a Pt nanoparticle-loaded carbon nanofiber electrode for hydrogen peroxide sensing. Biosensors and Bioelectronics. 26(11) (2011) 4585-4590.

[44] G. Maduraiveeran, & R. Ramaraj, Gold nanoparticles embedded in silica sol–gel matrix as an amperometric sensor for hydrogen peroxide. Journal of Electroanalytical Chemistry. 608(1) (2007) 52-58.

[45] J. Kolny, A. Kornowski, & H. Weller, Self-organization of cadmium sulfide and gold nanoparticles by electrostatic interaction. Nano Letters. 2(4) (2002) 361-364.

[46] M. Liu, R. Liu, & W. Chen, Graphene wrapped Cu_2O nanocubes: non-enzymatic electrochemical sensors for the detection of glucose and hydrogen peroxide with enhanced stability. Biosensors and Bioelectronics. 45 (2013) 206-212.

[47] B. Celik, Y. Yildiz, H. Sert, E. Erken, Y. Koskun, & F. Sen, Monodispersed palladium–cobalt alloy nanoparticles assembled on poly (N-vinyl-pyrrolidone)(PVP) as a highly effective catalyst for dimethylamine borane (DMAB) dehydrocoupling. RSC Advances. 6(29) (2016) 24097-24102.

[48] D.R. Dreyer, S.P. Ark, C.W. Bielawski, R.S. Ruoff, Chem. Soc. Rev. 39 (2010) 228.

[49] J.M. You, D. Kim, S.K. Kim, M.S. Kim, H.S. Han, & S. Jeon, Novel determination of hydrogen peroxide by electrochemically reduced graphene oxide grafted with aminothiophenol–Pd nanoparticles. Sensors and Actuators B: Chemical. 178 (2013) 450-457.

[50] (a) S.W. Ting, A.P. Periasamy, S.M. Chen, & R. Saraswathi, Direct electrochemistry of catalase immobilized at electrochemically reduced graphene oxide modified electrode for amperometric H_2O_2 biosensor. Int. J. Electrochem. Sci. 6 (2011) 4438-4453. (b) J.M. You, D. Kim, S.K. Kim, M.S. Kim, H.S. Han, & S. Jeon, Novel determination of hydrogen peroxide by electrochemically reduced graphene oxide grafted with aminothiophenol–Pd nanoparticles. Sensors and Actuators B: Chemical. 178 (2013) 450-457.

Professor Fatih Sen
Dumlupinar University
Department of Biochemistry
Kutahya/Turkey/43020

Tel: 90 274 265 20 31/ 3702
Fax: 90 274 265 20 20
E-mail: fatih.sen@dpu.edu.tr
http://senresearchgroup.com/

Highlights

- An easy and facile synthesis of monodisperse novel Pd/TNM@rGO nanocomposites
- Rapid, Sensitive, and Reusable Detection of H_2O_2 by novel nanocomposites
- The excellent electrochemical sensing properties of monodisperse Pd/TNM@rGO
- Thanks to the ultrasmall sizes, monodispersity and high Pd % surface of novel materials.